High-Index Materials for 193 nm Immersion Lithography

John H. Burnett*[a], Simon G. Kaplan[a], Eric L. Shirley[a], Paul J. Tompkins[b], and James E. Webb[b]

[a]NIST, 100 Bureau Dr., Gaithersburg, MD, USA 20899-8421;
[b]Corning Tropel Corporation, 60 O'Connor Rd., Faiport, NY USA 14450

ABSTRACT

193 nm immersion lithography optical projection systems using conventional UV optical materials and water as the immersion fluid, with planar lens/fluid interfaces, have a practical numerical aperture (NA) limit near 1.3. The bottleneck for pushing the NA further is the refractive index of the final lens element. Higher-index immersion fluids cannot alone give much improvement, because the NA is limited by the lowest material index. In this paper we consider the possibility of using novel high-index materials in the last lens element to get around this bottleneck and to push the NA limit to at least 1.5, while containing the lens system size and complexity. We discuss three classes of high-index ($n>1.8$), wide-band-gap, oxide-based materials that have the potential for being fabricated with optical properties appropriate for lithography optics: group-II oxides, magnesium-aluminum-spinel-related materials, and ceramic forms of spinel. We present theoretical calculations and experimental measurements of the optical properties of these materials, including intrinsic birefringence, and we assess their prospects.

Keywords: immersion lithography, 193 nm lithography, hyper NA, high index materials, MgO, MgAl$_2$O$_4$, spinel, ceramic spinel, intrinsic birefringence.

1. INTRODUCTION

Using water as the immersion fluid, 193 nm immersion lithography with numerical aperture (NA) near 1.3 now appears feasible.[1] To push the NA beyond this requires consideration of the refractive indices not only of the resist and the immersion fluid, but also of the final lens element. For plane-parallel lens/fluid and fluid/resist interfaces, by Snell's law, the NA is limited by the lowest index of the resist, the immersion fluid, and the final lens element. Because of the high fluence through the small last lens element, this element may be required to be made of crystalline material, e.g., calcium fluoride, with an index of 1.50 at 193 nm.[2] Water has an index of 1.44 at 193 nm,[3] but several laboratories have reported candidate higher-index immersion fluids with indices near 1.65.[4] Thus with the resist having an index 1.7 or above, the index of the final lens element may be the bottleneck for increasing the NA of the system, limiting the practical NA to near 1.3. A large curvature at the lens/fluid interface can in principle be used to get around this limit, but this may be impracticable.
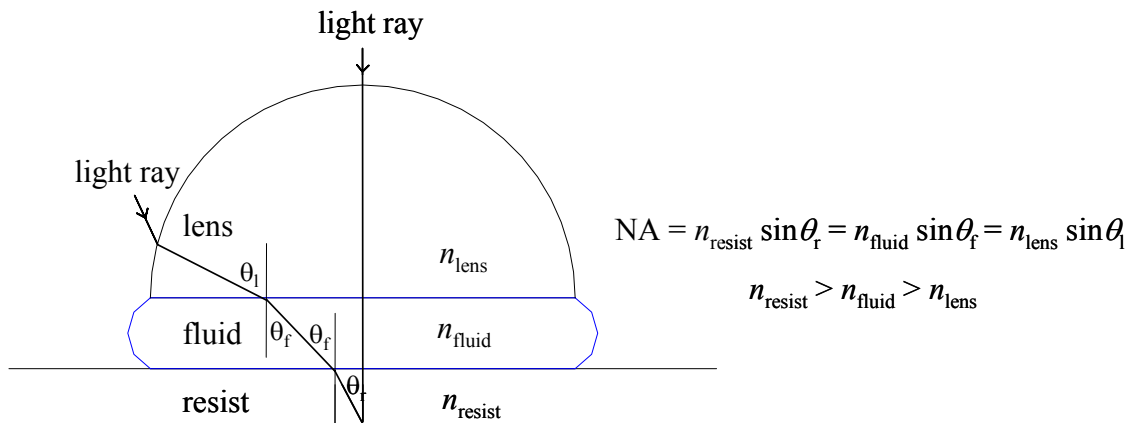

Fig. 1. Schematic of light rays traveling through final lens element, immersion fluid, and resist. The NA is limited by the smallest index.

$$NA = n_{resist} \sin\theta_r = n_{fluid} \sin\theta_f = n_{lens} \sin\theta_l$$

$$n_{resist} > n_{fluid} > n_{lens}$$

*Correspondence: Email: john.burnett@nist.gov; Tel: 301-975-2679

An alternative approach to pushing the NA above this limit is to use a lens material with a 193 nm index considerably higher than that of conventional UV optical materials.[5] With the smallest material index having a value of 1.65, for the equivalent dry NA pushed to 0.92, the immersion NA would be equal to 1.52. For λ=193 nm and assuming the theoretical limit for the k_1 factor of 0.25, the Rayleigh-criterion-resolution minimum half pitch would be Res_{min}=$k_1 \lambda$/NA=32 nm. With higher material indices, 32 nm could be achieved with a relaxed k_1 factor. Some optimism can be generated from recent results of good 32 nm line-and-space patterns for 2-beam interferometric exposure using an immersion fluid with an index n=1.64.[4]

In this paper we present a theoretical and experimental study of alternative UV high-index crystalline materials for 193 nm immersion lithography technology, and of their potential benefits. In Section 2 the impact of high-index materials on optical design, including NA and lens size reduction, will be explored with realistic simulations. In Section 3 we consider the requirements of candidate high-index materials, discuss three classes of high-index, wide-band-gap oxide materials that look promising, and present calculations and measurements of some of their key optical properties. In Section 4 we conclude with a discussion of the prospects for exploiting these high-index materials to extend the NA of immersion lithography optics beyond 1.3.

2. HIGH-INDEX SIMULATIONS

An important feature of the high-index-materials approach to increasing the NA limit is that the high-index materials only need to be used for the final small lens element (or perhaps last few elements) to achieve the NA gain. Further, a substantial NA gain can be achieved without increasing the lens size with the same design form. This is demonstrated by the ray-tracing simulation shown in Fig. 2. Fig. 2a) shows the marginal light rays through the last two elements of an immersion imaging system design with the final lens made of calcium fluoride (n=1.50) and water (n=1.44) as immersion fluid. For an equivalent dry NA of 0.9, near the practical limit, the NA limit of the immersion system is $\approx$1.3. Fig. 2b) shows the marginal light rays through the last two elements of a similar immersion imaging system design with the final lens made of a high-index material (n=1.87) and a high-index fluid (n=1.65) as immersion fluid. In this case, for an equivalent dry NA of 0.9, the NA limit of the system is $\approx$1.5. This NA increase is achieved with a similar aperture size. Thus for a lens system with a similar size and complexity, with a high-index material for the last lens element and using a high-index immersion fluid, an imagining resolution improvement of (1.3/1.5)$\approx$0.87 is obtained. This improvement cannot be achieved with the high-index fluid alone, because the NA is limited by the lowest material index. The role of the high index material here is to enable NA gains from the higher-index fluid and also to contain the lens sizes.
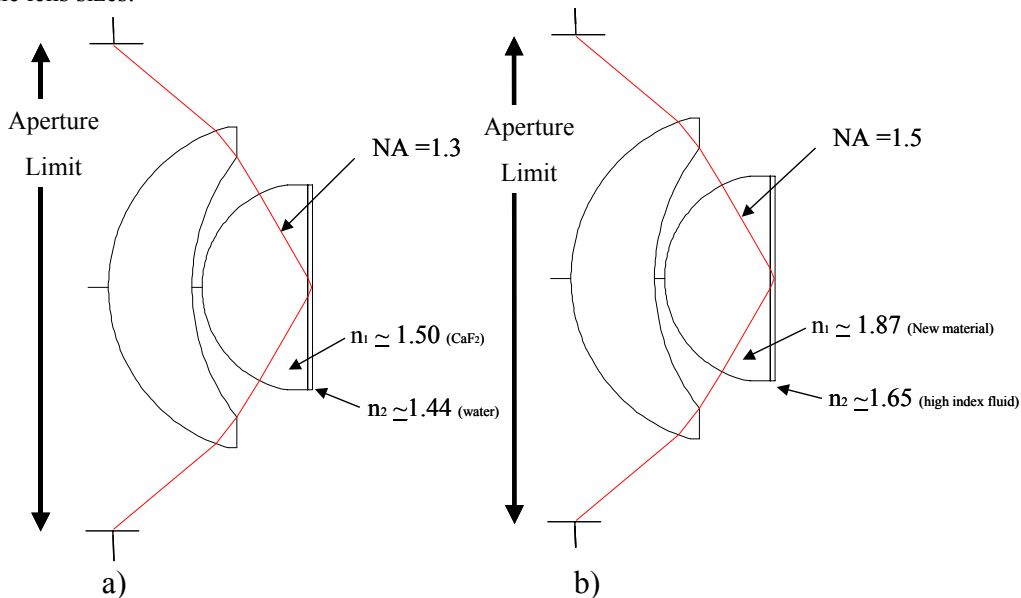

Fig. 2. a) Simulation of the marginal light rays for the final lens elements in an immersion system design with calcium fluoride (n=1.50) as last lens and water (n=1.44) as immersion fluid, showing a maximum practical NA of ~1.3. b) Simulation of the marginal light rays for the final lens elements in an immersion system design with a high-index material (n=1.87) as last lens and a high-index fluid (n=1.65) as immersion fluid, showing maximum practical NA of ~1.5, with the same aperture size.

To illustrate the impact of the high-index materials on lens system size, Fig. 3 below shows a ray-tracing simulation comparing two designs with the same NA. Fig. 3a) shows the same 1.3 NA system as Fig. 2a) above. Fig. 3b) shows a simulation for the case where the final lens is made of a high-index material (n=1.87), water is the immersion fluid, and where the NA is contained to be the same value NA=1.3 as 3a). In this case, for the same lens system complexity, the aperture size is reduced to about 80 % of the original aperture, approximately the ratio of the material indices. Thus this system delivers the same resolution, but has the lens size and complexity of a lower NA "dry" objective design.

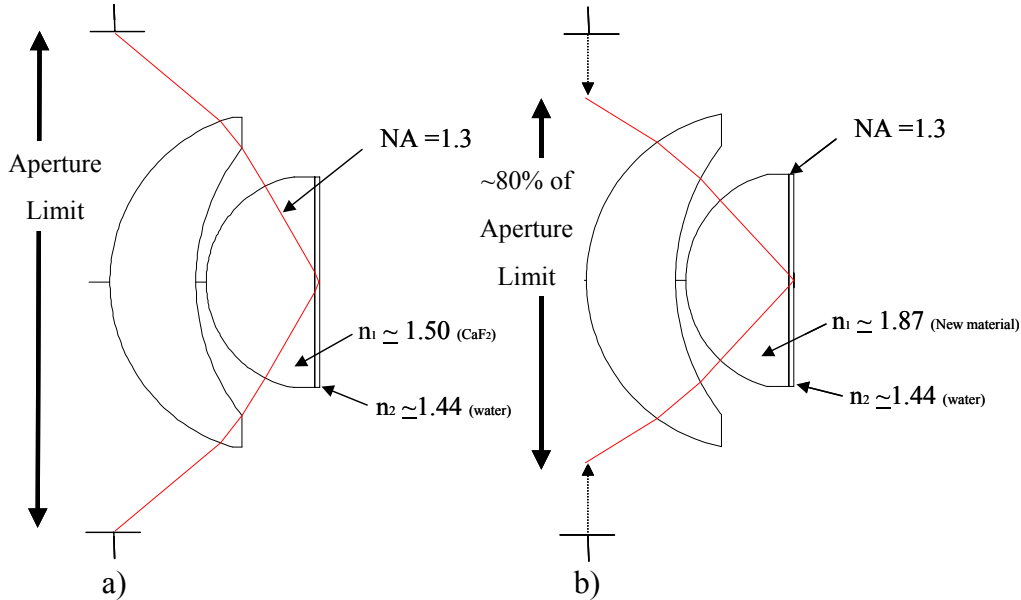
a)   b)

Fig. 3. a) Simulation of marginal light rays for the final lens elements in an immersion system design with calcium fluoride (n=1.50) as last lens and water (n=1.44) as immersion fluid, showing a maximum practical NA of ≈1.3. b) Simulation of the marginal light rays for the final lens elements in immersion system design with a high-index material (n=1.87) as last lens and water (n=1.44) as immersion fluid, and with the NA constrained to 1.3 as in 3a). This shows an aperture reduction of about 80 %.

3. CANDIDATE HIGH-INDEX MATERIALS

Do practical high-index materials exist that could be made with the size and quality required for lithography optics? At present no high-index material meets the tight lithography specifications, nor for that matter does any material besides fused silica and calcium fluoride. Very considerable effort was required to develop these materials to their present high quality. However, there are materials with substantially higher index than that of fused silica and calcium fluoride, that have electronic band gaps sufficiently high that they could in principle have high transmission at 193 nm. These materials would certainly have to undergo a development program, but the potential high payoff makes them worth considering.

A credible candidate material must have hope of achieving a number of very stringent specifications. 1) It must have high transmittance at 193 nm. The specification would of course be design-dependent, but a rough minimum transmittance requirement, assuming a final 3 cm thick lens, might be ≈90 %. This requires an absorption coefficient (base 10) of $A_{10} \leq 0.015$. 2) The refractive index would have to be high enough to be worth the effort, say as high as that of the resist ≥ 1.70. 3) The material would have to have isotropic optical properties, thus it would either have to have cubic crystal structure or be amorphous or polycrystalline. 4) The material would ultimately have to be capable of being made with lithography-grade optical quality, e.g., have good index homogeneity, i.e., $\Delta n \leq 1$ ppm, and low stress-induced birefringence, ≤ 1nm/cm. The relatively small path length through the lens may relax these requirements somewhat, but the criticalness of the final lens may tighten them. 5) Any intrinsic birefringence of the material would have to be small enough to be manageable in the design.[6,7] There are three ways that the intrinsic birefringence can be dealt with: First, if the material is amorphous or polycrystalline, the effect may be absent or small enough to be neglected. Second, if the value is small enough, its effects may be minimized in the design, e.g., by clocking lens crystal axis orientations. Finally, some mixed solid solution of materials with opposite signs of the intrinsic birefringence may

found such that the value is nulled out, e.g., as the intrinsic birefringence was shown to be nulled out for $Ca_{0.3}Sr_{0.7}F_2$ at 157nm.[5]

What are the materials possibilities, starting with trying to satisfy the first two above requirements at 193 nm, high transmission and high index? A necessary requirement for high transmission at 193 nm is that the electronic band gap of the material be considerably higher than the energy corresponding to this wavelength, namely 6.41 eV (193.4 nm). A substantial gap between the band edge and the photon energy is necessitated by the exponential Urbach absorption tail extending below the gap and by the ubiquitous shallow impurity states near the band edges. A relatively large solid band gap generally requires large ionicity. A high index requires high polarizability, thus high valence electron density, and thus small ionic radii. Satisfying both these conditions tends to restrict the possibilities to solids made from elements from Group I or Group II of the periodic table with elements near the top of Group VI or Group VII, namely the Group I or Group II fluorides, or Group II oxides. The Group I fluorides tend to be highly water soluble. The Group II fluorides, e.g., BeF_2, MgF_2, CaF_2, SrF_2, and BaF_2, are well known UV optical materials. All have absorption edges well above 6.41 eV, in fact too far above this energy for the index to be high there. The highest index of this group is that of BaF_2, with n=1.57 at 193 nm.[8] By substituting oxygen for fluorine, the band gap lowers somewhat and the anions are more polarizable, which tends to drive the index up. The result is that Group II oxides and related materials generally have considerably higher indices at 193 nm, while still having band gaps above the 193 nm photon energy. We will now discuss three classes of high-index oxide materials that may have promise for 193 nm lithography optics applications. We have made initial characterizations of the optical quality of these materials through measurements of the transmittance and residual birefringence. These properties in principle can be improved through higher-purity starting raw materials, optimized growth parameters, and post-growth treatment. To assess their potential suitability for high-index 193 nm lithography optics, we focused on the intrinsic properties of index dispersion, thermo-optic coefficient, and intrinsic birefringence.

3.1 Alkaline earth oxides

The Group II elements Mg, Ca, Sr, and Ba form a series of high-index cubic oxides, MgO, CaO, SrO, and BaO, with decreasing band gap energies, respectively. MgO, is the only one with a band gap, 7.6 eV,[9] higher than 6.41 eV. MgO (periclase) and CaO (lime) have rocksalt crystal structure and form a mixed solid solutions $Ca_xMg_{1-x}O$ for x in the range 0 to 0.1,[10] with the band gap expected to be greater than 6.41 eV over this range. Due to their high melting points $(M_p^{MgO}=2800\ °C)$, these oxides are often grown as crystals by an arc-fusion method. MgO can be made as large (> 7 cm diameter) single-crystal ingots, and is used commercially for substrates because of its thermomechanical properties. From the literature, the most UV-transparent MgO materials have substantial impurity absorption below the band edge. The material with the smallest absorption coefficient (base 10) at 193 nm we are aware of has A_{10}=3.9 cm^{-1}.[11]
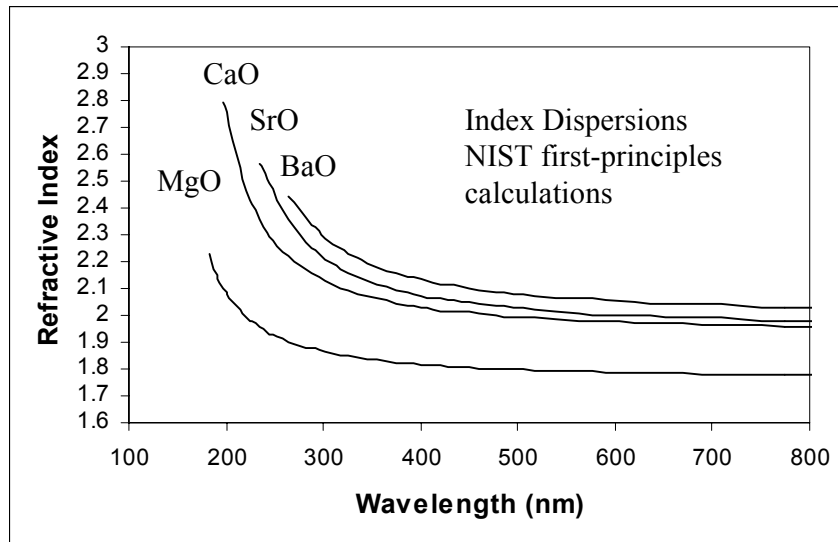

Fig. 4. Preliminary first-principles calculations of the index dispersions of MgO, CaO, SrO, and BaO for wavelengths from the visible down to near their band edge energies in the UV.

In Fig. 4 we present our preliminary first-principles calculations of the index dispersion for these oxides down to near their expected band edges in the UV.[6] The calculations indicate that MgO should have an index of n=2.1 near 193 nm and that mixing in of CaO should increase the index.

We obtained a single-crystal sample of MgO from Commercial Crystal Laboratories, in Naples, Florida. The sample was in the form of a rectangular parallelepiped, with (100) cleaved faces, about 10 mm on a side. To characterize the quality of the material we measured the transmittance and residual birefringence. A transmittance spectrum of this sample, through a 9 mm thickness, is shown in Fig. 5. The spectrum shows strong absorption below about 260 nm, probably due to impurities from the starting MgO power or introduced, e.g., by the electrodes, in the arc-fusion-growth process. We are now performing trace-impurity analysis on this material to identify the impurities and to attempt to establish the source. We measured the residual birefringence of the MgO sample at 633 nm using a Exicor 450AT photoelastic-modulator-based polarimeter from Hinds Instruments.[†] The birefringence magnitude over the sample, excluding the edges, had an average value of 10.3 nm/cm, with a standard deviation of 4.5 nm/cm.
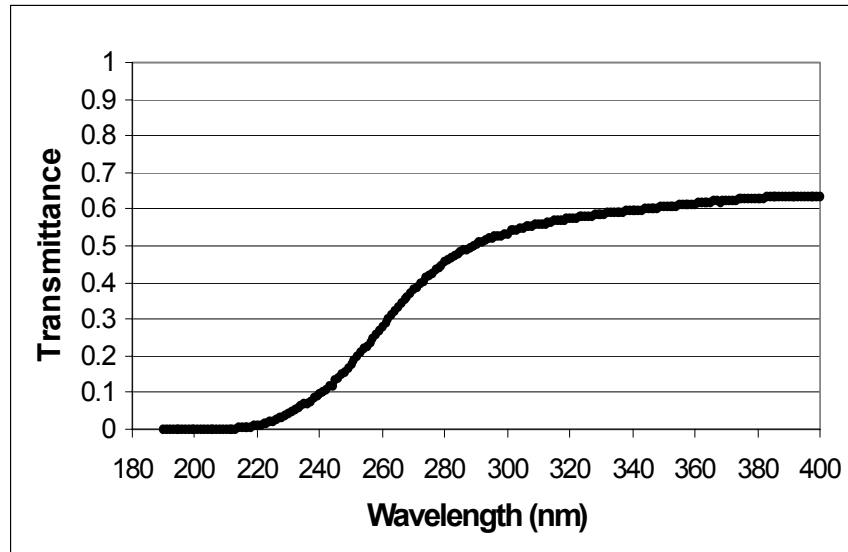

Fig. 5. Measured transmittance spectrum of MgO through a thickness of 9 mm.

We determined the index dispersion of the sample by ellipsometry, using a VUV-VASE spectroscopic ellipsometer from J. A. Woolam Co.[†] From the ellipsometric data Δ and ψ, we directly calculated the index in the range 800 nm to 140 nm. The resulting index dispersion is shown in Fig. 6, which gives an index value for MgO at 193 nm of 1.96. The data comes from a surface measurement, so it would be expected that the measured value of the index should depend on the surface conditions. Measurements with different surface preparations indicated an index uncertainty near 193 nm of about 5%.

A key property of a crystalline material for precision UV optics is the magnitude of the intrinsic birefringence. We measured this by determining the orientation of the crystal axes [110], [−110], and [001] in the sample, propagating light in the [−110] direction, and determining the relative phase shift developed for polarizations in the [001] and [110] directions, using a phase compensator.[6] Since the material was highly absorbing below 260 nm, we were only able to make this measurement down to 254 nm. This result is presented in Table 1, along with a measurement at 365 nm. By comparing our first-principles calculation of the effect with the measured values at 365 nm and 254 nm, we estimate a nonlinear extrapolation of the measured values to 193 nm to be roughly 70 nm/cm. Our experience with comparing our calculations of intrinsic birefringence with measurements suggests that this extrapolation should be good to about 20%, but of course we caution that extrapolation into a divergent region is very risky. We have yet to measure intrinsic birefringence for CaO. However, it is possible that the sign and magnitude of the intrinsic birefringence of CaO may enable a nulling of the intrinsic birefringence at 193 nm in a mixed solid solution $Ca_xMg_{1-x}O$, in a way similar to how the mixture $Ca_{0.3}Sr_{0.7}F_2$ nulled it at 157nm.[5]
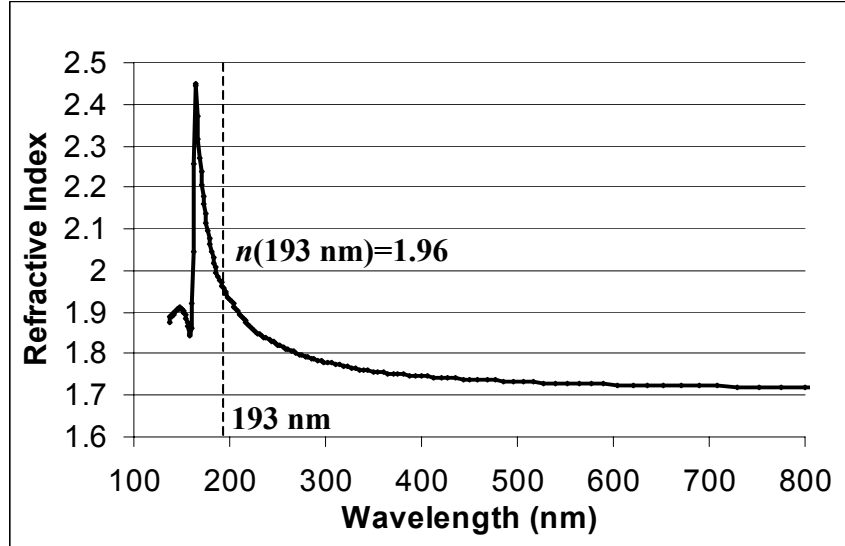
Fig. 6. Measurement of the index dispersion of MgO for wavelengths 800 nm to 140 nm, from spectroscopic ellipsometry.

The significance of a magnitude of the intrinsic birefringence of MgO at 193 nm of near 70 nm can be appreciated by comparison to that of CaF_2 at this wavelength. For CaF_2, the measured value of 3.4 nm/cm at 193 nm[6] is sufficiently large to have an impact on 193 nm system optics design, generally requiring ameliorating design approaches, such as crystal-axis clocking between CaF_2 elements.

Table 1. Measured magnitude of intrinsic birefringence of MgO (193 nm value extrapolated)

Wavelength	365.1 nm	253.7 nm	193 nm
IBR (nm/cm)	3.6±0.2	16.0±0.5	Extrapolated: 70

3.2 Crystalline spinel

Aluminum forms a wide-band-gap, high-index oxide, Al_2O_3 (sapphire), but this material is uniaxial. However, with the addition of Mg, one can form cubic magnesium aluminum spinel $MgAl_2O_4$, a naturally occurring mineral and gem stone.[12] This crystal has face-centered cubic structure, with 8 formula units in the unit cell. Spinel is synthesized from MgO and Al_2O_3 powder using Czochralski, gradient furnace, and other techniques. The fundamental absorption edge (band-gap exciton) is near 7.75 eV (160 nm), so there is a possibility that this material can be made with high transmittance at 193 nm. In addition to the stoichiometric form of spinel, by changing the composition of the melt, spinel can be synthesized in forms from Mg-rich to highly Al-rich. In addition, with appropriate growth temperature and conditions, spinel can be grown with an inverse structure, where Mg and Al swap positions at some of the crystal sites. The composition and atomic-site-position variations in the spinel system potentially allow some manipulation of the optical properties, which may be of some benefit, e.g., to minimize the intrinsic birefringence. This should be explored.

We measured the optical properties of single-crystal stoichiometric $MgAl_2O_4$ obtained from Saint-Gobain Crystals, in Newbury, Ohio. From a single-crystal ingot 5 cm in diameter, we cut samples for transmittance measurements and cut crystallographically-oriented samples for intrinsic-birefringence measurements, as for our MgO measurements. A transmittance spectrum of a sample, through a 3.4 mm thickness, is shown in Fig. 7. The spectrum shows 30 % transmittance at 193 nm, corresponding to an absorption coefficient (base 10) of $A_{10} = 1.3$, accounting for a 15% reflectance loss. Impurities are also likely responsible for the sharp drop in transmittance below 200 nm.
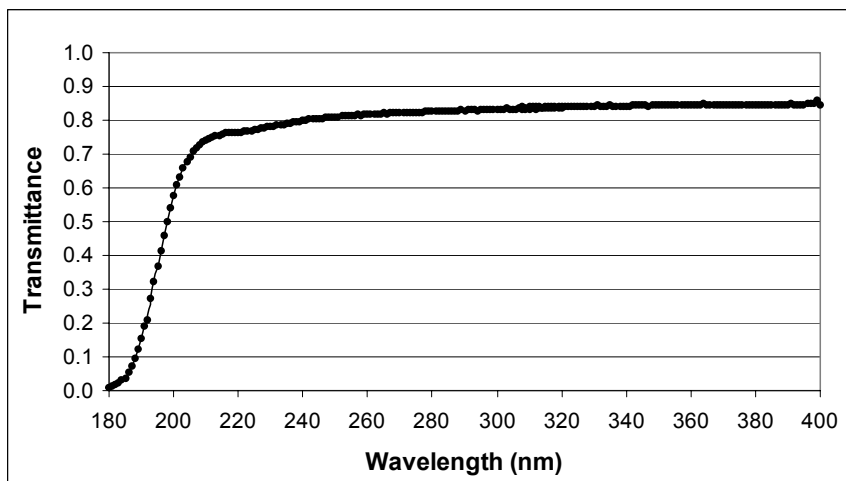
Fig. 7. Measured transmittance spectrum of $MgAl_2O_3$ through a thickness of 3.4 mm.

We determined the index dispersion of the sample by ellipsometry, by the same method we used for MgO. The index dispersion is shown in Fig. 8, which gives an index value for $MgAl_2O_4$ at 193.4 nm of 1.87.
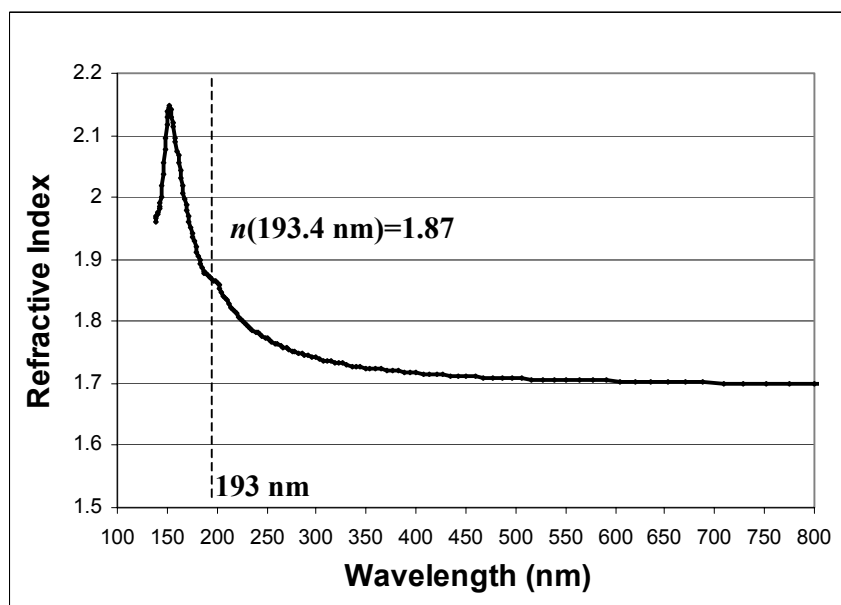

Fig. 8. Measurement of the index dispersion of $MgAl_2O_4$ for wavelengths 800 nm to 140 nm, from spectroscopic ellipsometry.

We measured the magnitude of the intrinsic birefringence on the oriented sample for wavelengths from 346 nm down to 195 nm, using the same method as for MgO. The wavelength dependence is displayed in Fig. 9, and the values are given in Table 2. The measured magnitude at 195 nm is 50.6 nm/cm. Linear extrapolation to 193.4 nm gives 52.0 nm/cm, fifteen times larger than that for CaF_2 at this wavelength.
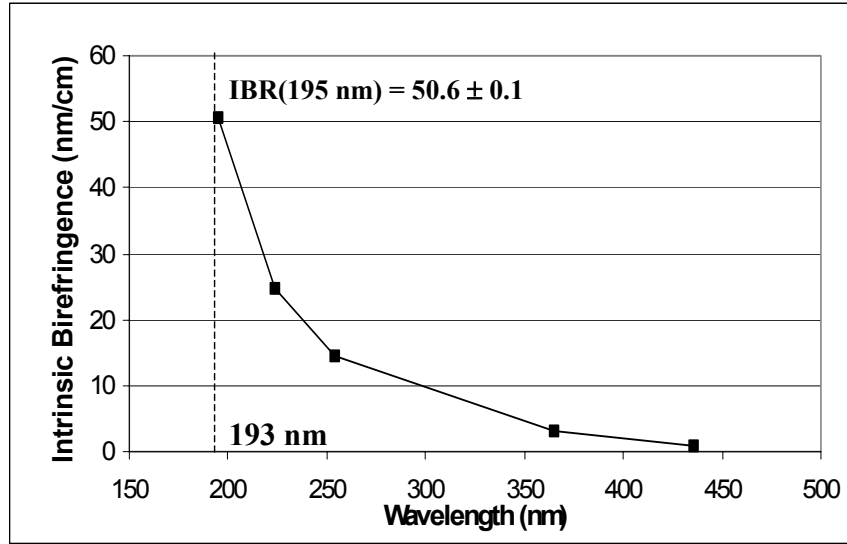
Fig. 9. Measurement of the intrinsic birefringence of $MgAl_2O_4$ for wavelengths down to 195 nm.

Table 2. Measured magnitude of intrinsic birefringence of $MgAl_2O_4$ (193.4 nm value extrapolated)

Wavelength	435.6 nm	365.1 nm	253.7	224.0	195 nm	193.4 nm
IBR (nm/cm)	0.94±0.05	3.14±0.05	14.6±0.1	24.7±0.1	50.6±0.1	Extr: 52.0

3.3 Ceramic spinel

Magnesium aluminum spinel can also be made into an isotropic polycrystalline ceramic by high-temperature/high pressure fusing of spinel powder.[13] By this inexpensive sintering process, large plates, >30 cm in dimension and >2 cm thick can be fabricated. The material can be optically transparent and very hard, and is being developed for transparent armor. The size of the crystal grains is typically ~10 μm, but the grain size can be controlled and reduced by appropriate growth conditions. A SEM cross section of a ceramic spinel sample (from Technology Assessment & Transfer Inc. (TA&T), in Annapolis, Maryland), thermally etched to reveal grain boundaries, showing a distribution of grain sizes, is presented in Fig. 10.
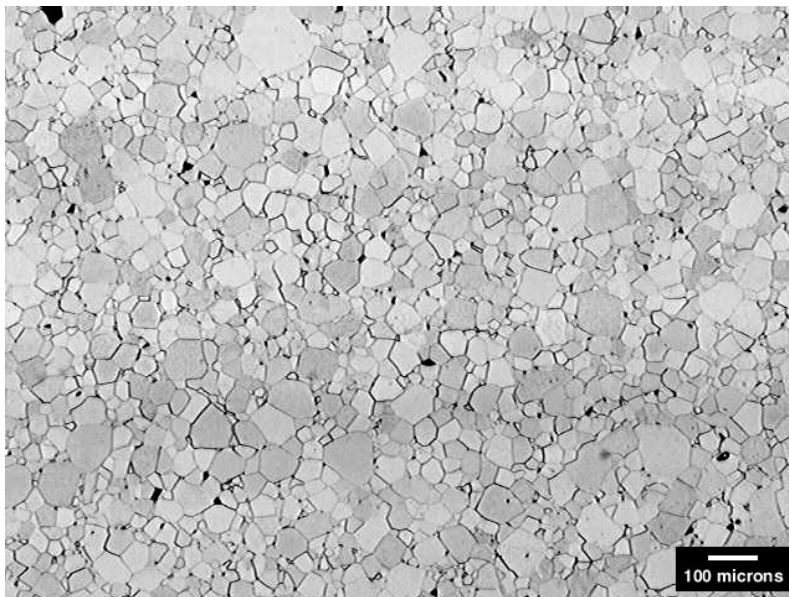

Fig. 10. Polished SEM cross section thermally etched to reveal grain boundaries.

The material has been developed for visible and infrared optics applications, but because it is made of fused spinel grains, UV transmission nearly as high as that of crystalline spinel should be possible. Further, because of the small, randomly-oriented crystal grains, the material should be substantially free of the intrinsic birefringence of single crystals, though some random depolarization effects should result due to the large intrinsic birefringence in the individual grains. This needs to be explored.

We characterized some of the optical properties of ceramic spinel samples provided by TA&T. A transmittance spectrum of a 2.7 mm-thick sample is shown in Fig. 11. The spectrum shows about 20% transmission at 193 nm, corresponding to an absorption coefficient (base 10) of $A_{10} = 2.3$, accounting for a 15% reflectance loss. The spectrum shows an absorption peak at ~210 nm. We are now performing trace impurity analysis on this material to identify the impurities responsible for this absorption.
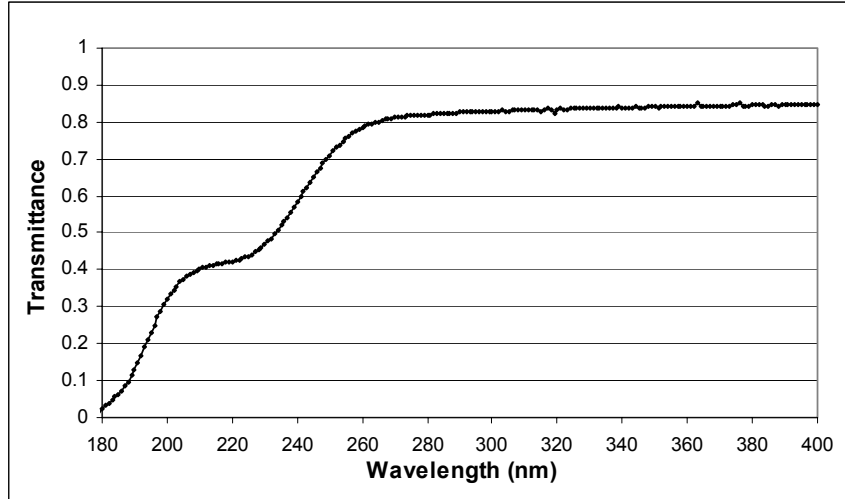

Fig. 11. Measured transmittance spectrum of ceramic spinel through a thickness of 2.7 mm.

We also measured the residual birefringence of the ceramic spinel sample at 633 nm. The birefringence magnitude over the sample, excluding the edges, had an average value of 5.3 nm/cm, with a standard deviation of 3.2 nm/cm. The center half of the sample (6 mm diameter area) had a birefringence average value of about 1 nm/cm.

We measured the index of refraction and the thermo-optic coefficient at 193 nm and at 20.15 °C by the minimum-deviation method.[2] The values, also listed in Table 3, are: 1.91 and 86×10^{-6}/°C, respectively. For comparison, the thermo-optic coefficient for CaF_2 and for water at 193 nm are -2.9×10^{-6}/°C and -100×10^{-6}/°C, respectively.[2,3]

Table 3. Measured index properties of ceramic spinel at 193 nm

Index(193.4 nm, 21.5 °C)	dn/dT(193.4 nm, 21.5 °C)
1.91±0.01	$+86(\pm10) \times 10^{-6}$/°C

4. CONCLUSIONS

We have identified three classes of oxide materials that are possible candidates for high-index optical materials which may be useful for final optical components of 193 nm immersion lithography optics to extend to NAs above 1.3. These classes are the Group II oxides (especially MgO), $MgAl_2O_4$ and its compositional and atomic-site variants, and ceramic forms of spinel. All can be grown in large sizes, with MgO and $MgAl_2O_4$ as single crystals and ceramic spinel as isotropic polycrystals. All have high indices, ~1.9, due in large part to the high polarizability of oxygen. All have band gaps above the 193 nm photon energy, enabling the possibility of high transmission at 193 nm. The relative nearness of the band edges to the 193 nm photon energy also contributes to the high indices. However, this nearness also gives rise to large values of other less desirable optical properties, which are generally also divergent near the band edges, e.g., the intrinsic birefringence and the thermo-optic coefficient.

Initial measurements of transmittance at 193 nm on available samples of these materials have shown that none are nearly transparent enough at 193 nm to be useful with their present quality. This is likely impurity related, and there is a good chance that the transmittance can be improved sufficiently with higher-purity starting raw materials and optimized growth processes. Other properties, such as stress-induced birefringence, need improvement as well. Some intrinsic properties, such as 193 nm index and intrinsic birefringence have been established.

The three classes have different characteristics related to their prospects:

MgO has the highest index at 193 nm, but also probably has the highest intrinsic birefringence. However, mixed-solid-solutions of the Group II oxides may provide the possibility of nulling or reducing the intrinsic birefringence. This material is the hardest to grow, due to its high melting point. It probably is the least mature as an optical material of the candidates, and thus it may have the most opportunity for further improvement.

Crystalline spinel is a well-established optical material, with relatively high-optical quality in the UV. The best material has the highest 193 nm transmission of the three classes. Spinel has a high intrinsic birefringence, but the wide phase space of compositional and atomic-site variants of spinel may provide the opportunity for tailoring of optical properties, e.g., minimizing the intrinsic birefringence. This needs to be explored.

Ceramic forms of spinel are probably the easiest to grow in quantity and have a manufacturing base for visible and infrared applications. The relatively high 193 nm transmission comes as somewhat of a surprise, as well as its low stress-induced birefringence. The randomly oriented polycrystalline nature of the material would be expected to eliminate the systematic intrinsic birefringence. However, due to the intrinsic birefringence in the individual grains, the depolarization properties at short wavelengths may be an issue. The polycrystalline nature and the grain boundaries give concern for scattering and index homogeneity. In principle, these issues could decrease with grain size, but the accompanying increase in grain boundary area (poor quality material) to grain volume, along with other growth trade-offs, may limit the benefits of this. Scattering and index homogeneity issues need to be explored.

Other oxide materials, e.g. garnets, are potential candidates. Yittrium aluminum garnet (YAG) is a well-established, high-quality optical material used for laser applications in the visible and in the infrared. Though the material is known to have absorption coefficients near 193 nm in the range of the other materials discussed,[14] the band edge energy 6.50 eV appears to be too close to the 193 nm photon energy 6.41 eV to allow much room for improvement. However, there are other related garnets with higher band gaps, which should be explored.

All of these materials have potential to meet the required specifications - it is all a matter of improving the UV optical quality. It should be noted that none of these materials have yet been grown with a focus on UV properties, and it seems that nonetheless their UV the properties are reasonably good. This generates some optimism. To achieve the tight lithography optics specifications, these or other oxide materials will require substantial material development programs. However, if these can be tackled successfully, the high-index-materials immersion approach presents a relatively easy route to an NA of 1.5 or higher. This offers the credible possibility of 32 nm feature sizes *with little or no increase in the size or significant increase in complexity of the system optics*. Considering the potentially high payoff, this materials effort may be well worthwhile.

[†] Certain commercial equipment, instruments, materials, or software are identified in this paper to adequately specify the experimental procedure. Such identification does not imply recommendation or endorsement by the National Institute of Standards and Technology, nor does it imply that the items identified are necessarily the best available for the purpose.

REFERENCES

1. Soichi Owa, Hiroyuki Nagasaka, Yuuki Ishii, Osamu Hirakawa, Taro Yamamoto, "Feasibility of immersion lithography," in *Optical Microlithography XVII*, edited by Bruce W. Smith, Proceedings of SPIE Vol. 5377 (SPIE, Bellingham, WA, 2004) 264-272.
2. Rajeev Gupta, John H. Burnett, Ulf Griesmann, and Matthew Walhout, "Absolute refractive indices and thermal coefficients of fused silica and calcium fluoride near 193 nm," Applied Optics **37**, 5964-5968 (1998).
3. John H. Burnett and Simon G. Kaplan, "Measurement of the refractive index and thermo-optic coefficient of water near 193nm," Journal of Microlithography, Microfabrication, and Microsystems **3**, 68-72 (2004).
4. T. Miyamatsu, Y. Wang. M. Shima, S. Kusumoto, T. Chiba, H. Nakagawa, K. Hieda, and T. Shimokawa, "Material design for immersion lithography with high refractive index fluid," to be published in Proceedings of SPIE, 5753-03 (2005).
5. John H. Burnett, Simon G. Kaplan, Eric L. Shirley, and James E. Webb, "High index materials for 193 nm and 157 nm immersion lithography," in *International Symposium on Immersion & 157 nm Lithography*, Walt Trybula, Ed., International SEMATECH, Austin TX (2004).
6. John H. Burnett, Zachary H. Levine, and Eric L. Shirley, "Intrinsic birefringence in calcium fluoride and barium fluoride," Phys. Rev. B **64**, 241102(R) (2001).
7. John H. Burnett, Zachary H. Levine, Eric L. Shirley, and John H. Bruning, "Symmetry of spatial-dispersion-induced birefringence and its implications for CaF_2 ultraviolet optics," Journal of Microlithography, Microfabrication, and Microsystems **1**, 213-224 (2002).
8. Michael E. Thomas and William J. Tropf, "Barium Fluoride (BaF_2)," in *Handbook of Optical Constants of Solids III*, edited by E. D. Palik (Academic Press, New York, 1998), 683-699.
9. David M. Roessler and Donald R. Huffman, "Magnesium Oxide (MgO)," in *Handbook of Optical Constants of Solids II*, edited by E. D. Palik (Academic Press, New York, 1998), 919-955.
10. Crystal Structure Data of Inorganic Compounds, Landolt-Bornstein, New Series Vol III/7b, edited by W. Peis and A. Weiss (Springer-Verlag, Berlin, 1975) p. 33.
11. C. Ballesteros, R. Gonzalez, S. J. Pennycook, and Y. Chen, "Optical and analytical transmission-electron-microscopy studies of thermochemically reduced MgO crystals," Phys. Rev. B **38**, 4231-4238 (1988).
12. William J. Tropf and Michael E. Thomas, "Magnesium Aluminum Spinel ($MgAl_2O_4$)," in *Handbook of Optical Constants of Solids II*, edited by E. D. Palik (Academic Press, New York, 1998), 883-897.
13. Mark C. L. Patterson, Anthony A. DiGiovanni, Larry Fehrenbacher, and Don W. Roy, "Spinel: Gaining Momentum in Optical Applications," in *Window and Dome Technologies VIII*, edited by Randal W. Tustison, Proceedings of SPIE Vol. 5078 (SPIE, Bellingham, WA, 2003) 71-79.
14. M. E. Innocenzi, R. T. Swimm, M. Bass, R. H. French, and M. R. Kokta, "Optical absorption in undoped yttrium aluminum garnet," J. Appl. Phys. 68, 1200-1204 (1990).